

Optimal driving field for multipartite quantum battery coupled with a common thermal bath

Z Q Yang(杨梓骞), L K Zhou(周立坤), Z Y Zhou(周正阳), G R Jin(金光日), L Cheng(程龙), and X G Wang(王晓光)
Citation: Chin. Phys. B, 2023, 32 (**11**): 110301. DOI: 10.1088/1674-1056/acdc12
Journal homepage: http://cpb.iphy.ac.cn; http://iopscience.iop.org/cpb

What follows is a list of articles you may be interested in

Generalized uncertainty principle from long-range kernel effects: The case of the Hawking black hole temperature

Rami Ahmad El-Nabulsi and Waranont Anukool
Chin. Phys. B, 2023, 32 (**9**): 090303. DOI: 10.1088/1674-1056/acac15

An efficient multiparty quantum secret sharing scheme using a single qudit

Wenwen Hu(胡文文), Bangshu Xiong(熊邦书), and Rigui Zhou(周日贵)
Chin. Phys. B, 2023, 32 (**8**): 080303. DOI: 10.1088/1674-1056/aca391

Lorentz quantum computer

Wenhao He(何文昊), Zhenduo Wang(王朕铎), and Biao Wu(吴飙)
Chin. Phys. B, 2023, 32 (**4**): 040304. DOI: 10.1088/1674-1056/acad6a

Performance of phase-matching quantum key distribution based on wavelength division multiplexing technology

Haiqiang Ma(马海强), Yanxin Han(韩雁鑫), Tianqi Dou(窦天琦), and Pengyun Li(李鹏云)
Chin. Phys. B, 2023, 32 (**2**): 020304. DOI: 10.1088/1674-1056/ac6ee3

Pseudospin symmetric solutions of the Dirac equation with the modified Rosen—Morse potential using Nikiforov—Uvarov method and supersymmetric quantum mechanics approach

Wen-Li Chen(陈文利) and I B Okon
Chin. Phys. B, 2022, 31 (**5**): 050302. DOI: 10.1088/1674-1056/ac2f33

Optimal driving field for multipartite quantum battery coupled with a common thermal bath

Z Q Yang(杨梓骞), L K Zhou(周立坤), Z Y Zhou(周正阳),
G R Jin(金光日), L Cheng(程龙)†, and X G Wang(王晓光)‡

[1] *Physics Department, Zhejiang Sci-Tech University, Hangzhou* 310018, *China*
[2] *Zhejiang Institute of Modern Physics, Department of Physics, Zhejiang University, Hangzhou* 310027, *China*

(Received 27 April 2023; revised manuscript received 5 June 2023; accepted manuscript online 7 June 2023)

For a many-atom battery coupled with a common thermal bath, the useful energy is maximized at an optimal number of the atoms for a fixed harmonic driving field, i.e., the so-called optimal building block [see Chang *et al. New J. Phys.* **23** 103026 (2021)]. Here we consider the useful energy defined by the ergotropy and a continuous-wave driving field. For the single-atom case, we present analytical results of the increased energy and the ergotropy in the long-time limit (i.e., the steady-state ergotropy). It is found that there exists an optimal value of the driving-field strength. Such an observation holds for many-atom cases. Numerically, we show that the optimal strength increases linearly with the number N of the atoms. Using the optimal strength for each N, both the increased energy and the ergotropy increase monotonically with N.

Keywords: quantum mechanics, thermodynamics

PACS: 03.65.–w, 05.70.–a

DOI: 10.1088/1674-1056/acdc12

1. Introduction

Quantum batteries (QBs) are the simplest quantum systems that store and provide energy using quantum coherence and quantum entanglement in charging processes.[1–5] Starting from original ideas developed in Refs. [6,7], various quantum systems have been considered as candidates of QBs, including collective spins,[8,9] interacting spin chains,[10,11] collision model,[12–15] and mechanical flywheels.[16,17] Recently, Ferraro *et al.*[18] proposed a charging model of finite-N two-level atoms via collectively interacting with a single cavity mode (known as the so-called Dicke QB). Many-body entanglement created by the common cavity model leads to the quantum advantage in the charging power in comparison with that of charging of each atom by each sperate cavity mode.[18] Collective charging QBs have been proposed in cavity and waveguide QED setups,[19–22] and most recently demonstrated by using fluorescent organic molecules in a microcavity.[23]

Using a static drving[6,10,24–26] and a harmonic driving field[18–20,27] as the charger, one can also realize a semi-classical Dicke model (i.e., the so-called multipartite quantum battery), where quantum correlations among the spins can be achieved by coupling with a common thermal bath. Without the presence of the bath, Zhang *et al.*[28] have proposed finite-N two-level atoms as a large-spin battery and the harmonic field as a charger. Analytical solutions has been derived to obtain the maximum stored energy in the battery.[28] Most recently, Chang *et al.*[29] further investigated the collective interaction of the atoms with the common thermal bath. Due to the presence of the harmonic driving field and the bath, they find that the free energy variation in the steady state increases non-monotonically and reaches the maximal value at an optimal number of atoms $N_{\rm opt}$. This result is somewhat counter-intuitive, since the stored energy should increase with N.

Here we investigate the setup of the QB similar to Chang *et al.*[29] by considering a continuous-wave driving field (equivalently, the harmonic driving field with a rotating-wave approximation). We adopt the so-called ergotropy to quantify the useful energy stored in the QB.[30] For the single-atom case (i.e., the conventional charging protocol with $N = 1$), analytical result of the increased energy is derived to compare with the ergotropy at the long-time limit (i.e., the steady-state ergotropy). By maximizing the steady-state ergotropy, we obtain an optimal value of the driving-field strength, dependent on the temperature of the bath. Such an observation holds for the finite-N case. With a fixed driving strength, there exists the optimal number of atoms $N_{\rm opt}$. Similar to Chang *et al.*,[29] it implies that there exists an optimal building block for the multipartite quantum battery. However, if we adopt the optimal driving field for each N, we can show that both the increased energy and the ergotropy increase monotonically with N, as is expected.

2. Quantum battery system

Following Chang *et al.*,[29] we consider a multipartite battery consisting of N identical two-level atoms, which is driven by a continuous-wave driving field with the frequency ω. The total Hamiltonian is described by a semi-classical Dicke model

†Corresponding author. E-mail: lcheng@zstu.edu.cn
‡Corresponding author. E-mail: xgwang@zju.edu.cn

© 2023 Chinese Physical Society and IOP Publishing Ltd

as follows:

$$\hat{H} = \hat{H}_{\rm S} + \hat{V},$$
$$\hat{H}_{\rm S} = \omega_0 \hat{J}_z, \quad \hat{V} = \frac{\lambda}{2}(\hat{J}_+ {\rm e}^{-{\rm i}\omega t} + \hat{J}_- {\rm e}^{{\rm i}\omega t}), \tag{1}$$

where ω_0 is the transition frequency of the atoms and λ denotes the driving-field strength. The atoms are described by the collective atomic operators $\hat{J}_z = \sum_{i=1}^{N} \sigma_z^{(i)}/2$ and $\hat{J}_+ = \sum_{i=1}^{N} |e\rangle_{ii}\langle g| = (\hat{J}_-)^\dagger$, with the Pauli operator $\sigma_z^{(i)} = |e\rangle_{ii}\langle e| - |g\rangle_{ii}\langle g|$. For brevity, we consider the resonance case, i.e., the driving frequency $\omega = \omega_0$. The battery state can be described by the Dicke states $\{|J,m\rangle\}$, with $J = N/2$ and $m = -J, -J+1, \ldots, +J$.

Next, we consider all the QBs (or the spins) weakly coupled with a common thermal bath, which provides an average number of excitations $\bar{n}(\omega_0) = 1/({\rm e}^{\beta\omega_0} - 1)$. For simplicity, we adopt the short-hand notation $\bar{n} = \bar{n}(\omega_0)$. After the long-time interactions, all the spins will be prepared in the Gibbs thermal state $\hat{\rho}_0$, i.e.,

$$\hat{\rho}(0) = \hat{\rho}_0 \equiv \frac{{\rm e}^{-\beta\hat{H}_{\rm S}}}{Z}, \quad Z = {\rm Tr}[{\rm e}^{-\beta\hat{H}_{\rm S}}], \tag{2}$$

where $\beta = 1/(k_{\rm B}T)$ is the inverse temperature, $k_{\rm B}$ is the Boltzmann constant, and the Z denotes the partition function. At the zero temperature ($T = 0$), we have the mean number of excitations $\bar{n} = 0$, the initial state corresponds to all the spins in the ground state $|g\rangle$, and therefore $E(0) = -N\omega_0/2$. With a finite temperature ($T \neq 0$), we obtain

$$E(0) = {\rm Tr}(\hat{\rho}_0\hat{H}_{\rm S}) = \omega_0\left[\bar{n} - \frac{N}{2} + \frac{1+N}{1-(1+1/\bar{n})^{1+N}}\right]. \tag{3}$$

For the single-atom case ($N = 1$), it reduces to $E(0) = -\omega_0/(2\chi)$, with $\chi = 2\bar{n}+1$.

To quantify the total energy stored in the QBs, we define the increased energy

$$\Delta E(t) = E(t) - E(0), \tag{4}$$

where $E(t) = {\rm Tr}(\hat{\rho}\hat{H}_{\rm S})$, with $\hat{\rho} = \hat{\rho}(t)$. According to Ref. [30], not all the energy can be extracted by unitary operations. The useful energy stored in the QBs is measured by the so-called ergotrogy[30]

$$W(t) = E(t) - {\rm Tr}(\hat{\sigma}_{\rm p}\hat{H}_{\rm S}), \tag{5}$$

with $\hat{\sigma}_{\rm p} = \sum_m \varepsilon_m |\psi_m\rangle\langle\psi_m|$ being the so-called passive state. Here $\{|\psi_m\rangle\}$ denotes the eigenvectors of $\hat{H}_{\rm S}$ and $\{\varepsilon_m\}$ represents the eigenvalues of $\hat{\rho}$ sorted in ascending order $\varepsilon_{m+1} \geq \varepsilon_m$. Note that the free energy $F = E - S/\beta$ has been used to quantify the useful energy stored in the battery (see e.g., Chang *et al.*[29]), where S is the entropy and β is the inverse temperature. Both of them obey the relation $F \geq W$,[30] with the equality holding for $N \to \infty$.[7,30]

3. Conventional charging protocol

Here, we first investigate the conventional charging protocol (i.e., the case of $N = 1$).[29] For this case, the spin operators in the Hamiltonians become $\hat{J}_+ \to \hat{\sigma}_+ = |e\rangle\langle g|$ and $\hat{J}_z \to \hat{\sigma}_z/2$. In the interaction picture, dynamics of the battery can be described by a Lindblad master equation (see Appendix A)

$$\frac{{\rm d}\hat{\rho}}{{\rm d}t} = -{\rm i}\frac{\lambda}{2}[\hat{\sigma}_x, \hat{\rho}] + \Gamma\bar{n}\left(\hat{\sigma}_+\hat{\rho}\hat{\sigma}_-^\dagger - \frac{1}{2}\{\hat{\rho}, \hat{\sigma}_-\hat{\sigma}_+\}\right) + \Gamma(\bar{n}+1)\left(\hat{\sigma}_-\hat{\rho}\hat{\sigma}_+^\dagger - \frac{1}{2}\{\hat{\rho}, \hat{\sigma}_+\hat{\sigma}_-\}\right), \tag{6}$$

where Γ denotes the damping rate, $[\hat{A}, \hat{B}] \equiv \hat{A}\hat{B} - \hat{B}\hat{A}$, and $\{\hat{A}, \hat{B}\} \equiv \hat{A}\hat{B} + \hat{B}\hat{A}$. Analytical expression of the energy is given by (see Appendix B)

$$E(t) = \omega_0\{a_1 + {\rm e}^{-\frac{3}{4}\chi\Gamma t}[b_1\cos(\Omega t) + c_1\sin(\Omega t)]\}, \tag{7}$$

where

$$a_1 = -\frac{\Gamma^2\chi}{2A^2}, \quad b_1 = -\frac{\lambda^2}{\chi A^2},$$
$$A = \sqrt{2\lambda^2 + \Gamma^2\chi^2}, \quad \chi = 2\bar{n}+1.$$

Other parameters can be found in Appendix B. Note that $E(0) = \omega_0(a_1 + b_1) = -\omega_0/(2\chi)$, as mentioned above. In Fig. 1(a), we show the increase energy $\Delta E(t)$ against t by taking a fixed driving-field strength $\lambda = 6\Gamma$ (the open circles), in exact agreement with the numerical results for $\bar{n} = 0$ (the red solid line), and 1 (the dashed line).

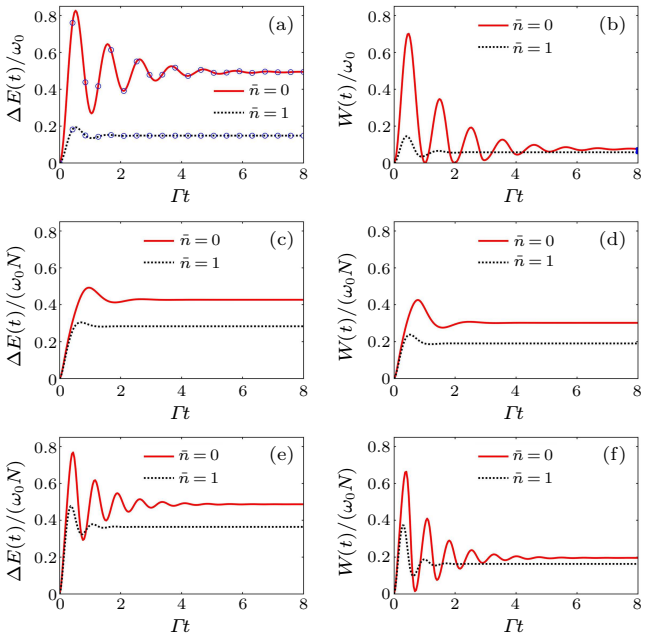


Fig. 1. (a)–(d) Time evolution of the increased energy $\Delta E/(\omega_0 N)$ and the ergotropy W for $N = 1$ (top) and $N = 10$ (middle) with a fixed driving-field strength $\lambda = 6\Gamma$. (e) and (f) The dynamics for a relatively larger driving field $\lambda = 10\Gamma$ and $N = 10$. Different curves correspond to different values of $\bar{n}$, i.e., $\bar{n} = 0$ (red solid line) and $\bar{n} = 1$ (black dashed line). The open circles in (a) represent the analytical result given by Eq. (7). The other parameters are $\Gamma = 1$ and $\omega = \omega_0 = 1000\Gamma$.

From Fig. 1(a), one can see that the increase energy $\Delta E(t)$ shows damped oscillations and approaches to its associated steady-state value $\Delta E(\infty)/\omega_0 = [E(\infty) - E(0)]/\omega_0 \to -b_1$, where $E(\infty) = \omega_0 a_1$, as expressed by Eq. (7). Note that $\Delta E(\infty)$ increases monotonically with the increase of λ. Hereafter, we focus on the steady-state values of the energy and the ergotropy and adopt the short-hand notations $\Delta E = \Delta E(\infty)$ and $W = W(\infty)$.

In Fig. 1(b), we show the ergotrogy $W(t)$ against t by taking a fixed driving-field strength $\lambda = 6\Gamma$ for $\bar{n} = 0$ (the red solid line), 1 (the dashed line). At $t = 0$, the initial Gibbs state $\hat{\rho}_0$ is indeed the passive state, and thereby $W(0) = 0$. With the time evolution, the role of the driving field results in the damped oscillations of $W(t)$, which is smaller than $\Delta E(t)$ at each t. As $t \to \infty$, one can obtain analytical result of $\hat{\rho}(\infty)$, which in turn gives (see Appendix B)

$$\frac{W}{\omega_0} = \frac{\sqrt{\chi^2 + (2\lambda/\Gamma)^2} - \chi}{2(A/\Gamma)^2}, \tag{8}$$

where χ and A have been defined in Eq. (7) and below. For a fixed $\lambda = 6\Gamma$, our numerical results show that the steady state appears at the time $\Gamma t \gtrsim 8$, with $W/\omega_0 \approx 0.09$ ($\bar{n} = 0$) and 0.063 ($\bar{n} = 1$), as shown in Fig. 1(b).

Maximizing Eq. (8) with respect to λ, we obtain

$$\lambda_{\rm opt} = \chi\Gamma\sqrt{\frac{1+\sqrt{2}}{2}}, \tag{9}$$

and therefore, the optimal value of the ergotropy

$$\frac{W_{\rm opt}}{\omega_0} \equiv \frac{W(\infty)|_{\lambda=\lambda_{\rm opt}}}{\omega_0} = \frac{\sqrt{2}-1}{2\chi}, \tag{10}$$

which is independent of the damping rate Γ and decreases with the increase of χ (also $\bar{n}$). In Fig. 2(a), we show W/ω_0 as a function of λ/Γ for $\bar{n} = 0$ (the red solid), 1 (the dashed), and 2 (the green dot-dashed). From top to bottom, our numerical results show $W_{\rm opt}/\omega_0 \approx 0.207$, 0.069, and 0.041, at $\lambda_{\rm opt}/\Gamma \approx 1.099$, 3.296, and 5.493, respectively, in good agreement with our analytic results (open circles).

4. Quantum advantage of a collective charging protocol

For the finite-N case, we consider the collective charging protocol, where dynamics of the QBs is given by the Lindblad master equation (see Appendix A)

$$\frac{{\rm d}\hat{\rho}}{{\rm d}t} = -{\rm i}\lambda[\hat{J}_x, \hat{\rho}] + \Gamma\Big[\bar{n}\Big(\hat{J}_+\hat{\rho}\hat{J}_- - \frac{1}{2}\{\hat{\rho}, \hat{J}_-\hat{J}_+\}\Big) + (\bar{n}+1)\Big(\hat{J}_-\hat{\rho}\hat{J}_+ - \frac{1}{2}\{\hat{\rho}, \hat{J}_+\hat{J}_-\}\Big)\Big]. \tag{11}$$

The permutation symmetry of the atoms leads to a reduction of the dimension of Hilbert space from 2^N to $N+1$, where the QB state $\hat{\rho}$ is a mixture of the Dicke states $\{|j,m\rangle\}$. For the atoms initially prepared in the Gibbs thermal state, the internal energy is described by Eq. (3). As $N \to \infty$, the mean energy per atom becomes $E(0)/(\omega_0 N) \to -1/2$, similar to Ref. [29]. In Figs. 1(c) and (d), we take $N = 10$ and show the time evolution of $\Delta E(t)/(\omega_0 N)$ and $W(t)/(\omega_0 N)$. Both of them increase to their associated steady-state values as $\Gamma t \gtrsim 4$, more quickly than that of the single-atom case. However, it is also necessary to show how the observable damps to the steady state for a large value of driving filed strength. In Figs. 1(e) and (f), we show the dynamics for a relatively larger driving strength (e.g., $\lambda = 10\Gamma$). One can see that the evolution time to the steady state becomes larger (i.e., $\Gamma t \gtrsim 8$). To obtain reasonable steady-states solutions for different values of $(N, \lambda/\Gamma)$, we adopt the steady-state solver of the QuTip, which has been widely used in the field of quantum optics.[31]

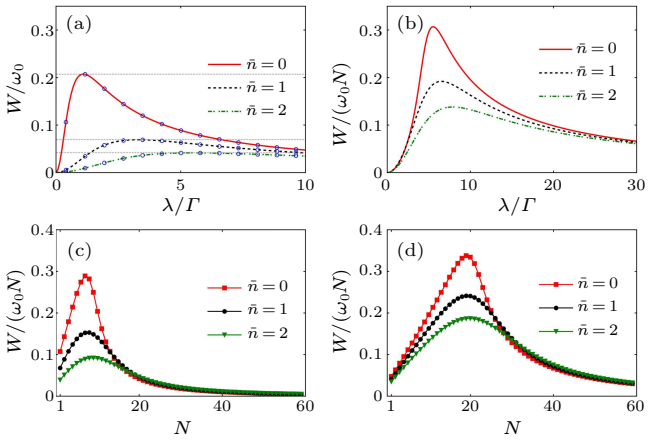


Fig. 2. The ergotropy per atom, $W/(\omega_0 N)$, for different atom numbers $N = 1$ (a), $N = 10$ (b), and driving-field strength $\lambda = 4\Gamma$ (c), $\lambda = 10\Gamma$ (d). (a) The hollow circles given by Eq. (8), the horizontal lines are the upper bound with the conventional charging protocol, which is given by Eq. (10). (c) and (d) The markers are numerical results and the lines are the fitting results. Different colors correspond to different values of $\bar{n}$, i.e., $\bar{n} = 0$ (red), $\bar{n} = 1$ (black), and $\bar{n} = 2$ (green). Parameters are $\Gamma = 1$ and $\omega = \omega_0 = 1000\Gamma$.

For the finite-N case, the ergotropy in the steady state depends on the driving-field strength (i.e., λ/Γ) and the mean thermal excitation number $\bar{n}$, i.e., $W = W(N, \lambda/\Gamma, \bar{n})$. In Fig. 2(b), we take $N = 10$ and show the ergotropy per atom $W/(\omega_0 N)$ as a function of λ/Γ for different values of $\bar{n}$. It yields non-monotonic relations between $W/(\omega_0 N)$ variation and λ/Γ. A peak with the maximal value of $W_{\rm opt}/(\omega_0 N)$ is observed at an optimal driving-field strength $\lambda_{\rm opt}$. We show that with the increase of the mean thermal excitation number $\bar{n}$, the ergotropy per atom $W/(\omega_0 N)$ and the maximal ergotropy per atom $W_{\rm opt}/(\omega_0 N)$ decease. One can see that there exists the optimal value of driving-field strengths, $\lambda_{\rm opt}/\Gamma$, which increases with $\bar{n}$. For example, $\lambda_{\rm opt}/\Gamma \approx 5.564$ ($\bar{n} = 0$), 6.541 ($\bar{n} = 1$), and 7.894 ($\bar{n} = 2$), respectively. Compared Figs. 2(a) and (b), the maximal ergotropy per atom, $W_{\rm opt}$, is better than the maximal ergotropy of the conventional charging case for $\bar{n} = 0$, 1 and 2.

In Figs. 2(c) and (d), we take two fixed driving-field strengths $\lambda = 4\Gamma$ and $\lambda = 10\Gamma$ to show $W/(\omega_0 N)$ as a function of N for different values of $\bar{n}$. One can see that there exists an optimal value of the number of the atoms $N_{\rm opt}$, similar to Chang *et al.*[29] This result is somewhat counter-intuitive, it implies that there exists an optimal building block for the multipartite quantum battery. As depicted by Fig. 2(c), one can see that $W/(\omega_0 N)$ increases with N and then decreases after $N_{\rm opt} = 7$ (for $\bar{n} = 0$), 8 ($\bar{n} = 1$), and 9 ($\bar{n} = 2$). For a larger driving-field strength (e.g., $\lambda = 10\Gamma$), Fig. 2(d) shows that $W/(\omega_0 N)$ reaches its maximum at $N = 19$, 19, and 20, respectively. Better than the single-atom case, the collective charging protocol shows an advantage within the quantum-enhancement region $1 < N \lesssim 2N_{\rm opt}$. Such an observation can be bypassed if one adopts the optimal driving field for each N.

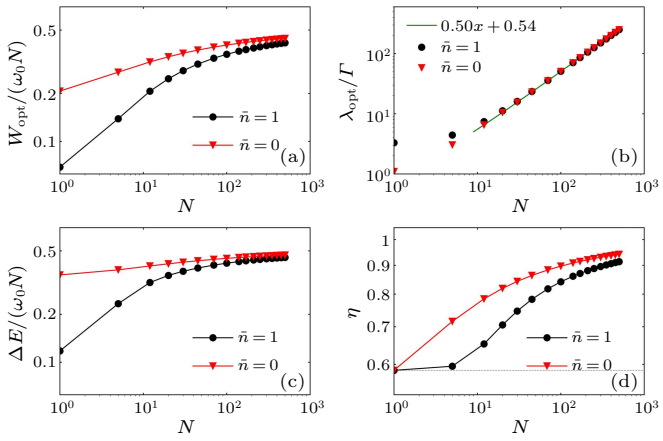


Fig. 3. (a) The maximal ergotropy per atom $W_{\rm opt}/(\omega_0 N)$, (b) the optimal driving-field strength $\lambda_{\rm opt}$, (c) the increased energy per atom $\Delta E/(\omega_0 N)$, and (d) the charging efficiency η varies over the number of atoms N. Different colors correspond to different values of $\bar{n}$, $\bar{n} = 0$ (red), and $\bar{n} = 1$ (black). (b) The green line is the fitting result of $\bar{n} = 0$. (d) The horizontal line indicates $\eta = 2 - \sqrt{2}$. Parameters are $\Gamma = 1$ and $\omega = \omega_0 = 1000\Gamma$.

In Fig. 3(a), we show $W_{\rm opt}/(\omega_0 N)$ as a function of N at the optimal driving-field strength $\lambda_{\rm opt}$. One can see that $W_{\rm opt}/(\omega_0 N)$ monotonically increases with N to its asymptotic value $1/2$, therefore the quantum enhancement is no longer constrained in an "optimal regime" as shown in Figs. 2(c) and (d). When N is small, the values of $\bar{n}$ have a great impact on the $W_{\rm opt}/(\omega_0 N)$, while such an effect of $\bar{n}$ is very weak when $N \gg 10^0$. In Fig. 3(b), we show $\lambda_{\rm opt}$ against N for different values of $\bar{n}$. Our numerical results show the linear relation $\lambda_{\rm opt} \propto N$ and vanishing influence of $\bar{n}$. In Fig. 3(c), we show the increased energy $\Delta E(\lambda_{\rm opt})/(\omega_0 N)$ against N. For the single-atom case, according to Eqs. (4) and (9), we can obtain the analytical relation between $\Delta E(\lambda_{\rm opt})/\omega_0$ and $\bar{n}$, i.e., $\Delta E(\lambda_{\rm opt})/\omega_0 = 1/(2\sqrt{2}\chi)$, which supports our numerical results $\Delta E(\lambda_{\rm opt})/\omega_0 \approx 0.354$ ($\bar{n} = 0$) and 0.118 ($\bar{n} = 1$). For multi-atom cases, $\Delta E(\lambda_{\rm opt})/(\omega_0)$ increases monotonically with N and tends to $1/2$, similar to the behavior of $W_{\rm opt}/(\omega_0 N)$.

In Fig. 3(d), we calculate the charging efficiency $\eta = W/\Delta E$ at the optimal driving-field strength, which measures the ratio of the useful energy to the total stored energy in the battery. Both the curves in Fig. (d) show the same efficiency ($\eta = 2 - \sqrt{2} \approx 0.586$) in the single-atom case ($N = 1$), which indicates that the charging efficiency η is not affected by the mean thermal excitation number $\bar{n}$. For multi-atom cases, the charging efficiency η monotonically increases with N and tends to 1 for different $\bar{n}$. Moreover, comparing the different colored curves, we find that the red curves ($\bar{n} = 0$) are always above the black ones ($\bar{n} = 1$) in Figs. 3(a), 3(c) and 3(d), therefore the mean thermal excitation number $\bar{n}$ has detrimental effects on $W_{\rm opt}/(\omega_0 N)$, $\Delta E(\lambda_{\rm opt})/(\omega_0)$, and η.

5. Conclusion

To summarize, we have investigated the multipartite quantum battery by considering a continuous-wave driving field and a common thermal bath. Different from Chang *et al.*,[29] we adopt the so-called ergotropy to quantify the useful energy stored in the QB. For the single-atom case (i.e., the conventional charging protocol), we present analytical results of the increased energy and the ergotropy at the long-time limit (i.e., the steady-state ergotropy). By maximizing the steady-state ergotropy, we obtain an optimal value of the driving-field strength, which is dependent on the temperature of the bath (or equivalently, the mean thermal excitation number $\bar{n}$). Such an observation holds for the finite-N case. With a fixed driving strength, we find that there exists the optimal number of atoms $N_{\rm opt}$, similar to Chang *et al.*[29] This implies that there exists an optimal building block for the multipartite quantum battery. If we adopt the optimal driving field with its strength dependent linearly with N, our numerical results indicate that both the increased energy and the ergotropy increase monotonically with N. Finally, we investigate the ratio of the useful energy and the total increased energy, which also depends on the temperature and the driving field. Using the optimal value of strength for each N, we find that the ratio also increases monotonically with N.

Appendix A: Lindblad master equation for the system

In the rotating frame with respect to ω, the total Hamiltonian is

$$\hat{H}_{\rm tot} = \frac{\delta}{2}\sum_j \hat{\sigma}_z^{(j)} + \frac{\lambda}{2}\sum_j \hat{\sigma}_x^{(j)} + \sum_k \omega_k \hat{b}_k^\dagger \hat{b}_k + {\rm i}\sum_{j,k} g_{j,k}\left(\hat{\sigma}_-^{(j)}\hat{b}_k^\dagger {\rm e}^{-{\rm i}\omega t} - {\rm H.c.}\right), \quad \text{(A1)}$$

where $\delta = \omega_0 - \omega$, $g_{j,k}$ is the coupling coefficient between the jth atom and the kth mode of the bath. Considering the resonant case, i.e., $\omega = \omega_0$ and hence $\delta = 0$, the Hamiltonian

becomes $\hat{H}_{\rm tot}=\hat{H}_0+\hat{V}_{\rm SR}$, where

$$\hat{H}_0=\frac{\lambda}{2}\sum_j\hat{\sigma}_x^{(j)}+\sum_k\omega_k\hat{b}_k^\dagger\hat{b}_k,$$
$$\hat{V}_{\rm SR}=\mathrm{i}\sum_{j,k}g_{j,k}\big(\hat{\sigma}_-^{(j)}\hat{b}_k^\dagger\mathrm{e}^{-\mathrm{i}\omega t}-\mathrm{H.c.}\big). \tag{A2}$$

In the interaction picture, we obtain

$$\tilde{V}_{\rm SR}(t)=\mathrm{e}^{\mathrm{i}\hat{H}_0t}\hat{V}_{\rm SR}\mathrm{e}^{-\mathrm{i}\hat{H}_0t}=\mathrm{i}\sum_{j,k}g_{j,k}(\tilde{\sigma}_-^{(j)}\hat{b}_k^\dagger\mathrm{e}^{-\mathrm{i}\Delta\omega_kt}-\mathrm{H.c.}),$$

where $\Delta\omega_k=\omega_0-\omega_k$ and

$$\tilde{\sigma}_\pm^{(j)}\equiv\mathrm{e}^{\mathrm{i}\hat{H}_0t}\hat{\sigma}_\pm^{(j)}\mathrm{e}^{-\mathrm{i}\hat{H}_0t}. \tag{A3}$$

Similarly, the reduced density matrix of the battery is given by

$$\tilde{\rho}_{\rm S}=\tilde{\rho}_{\rm S}(t)\equiv\mathrm{e}^{\mathrm{i}\hat{H}_0t}\hat{\rho}\mathrm{e}^{-\mathrm{i}\hat{H}_0t}. \tag{A4}$$

Following the standard method in quantum optics (see, e.g., Ref. [32]), we obtain the Lindblad master equation

$$\begin{aligned}\frac{\mathrm{d}\tilde{\rho}_{\rm S}}{\mathrm{d}t}=&\sum_{i,j,k}\Gamma_{ij}\Big\{\bar{n}(\omega_k)\Big(\tilde{\sigma}_+^{(i)}\tilde{\rho}_{\rm S}\tilde{\sigma}_-^{(j)}-\frac{1}{2}\{\tilde{\rho}_{\rm S},\tilde{\sigma}_-^{(i)}\tilde{\sigma}_+^{(j)}\}\Big)\\&+[\bar{n}(\omega_k)+1]\Big(\tilde{\sigma}_-^{(i)}\tilde{\rho}_{\rm S}\tilde{\sigma}_+^{(j)}-\frac{1}{2}\{\tilde{\rho}_{\rm S},\tilde{\sigma}_+^{(i)}\tilde{\sigma}_-^{(j)}\}\Big)\Big\}\\&+\mathrm{i}\sum_{i,j}\Lambda_{ij}\big\{[\bar{n}(\omega_k)+1][\tilde{\rho}_{\rm S},\tilde{\sigma}_+^{(i)}\tilde{\sigma}_-^{(j)}]\\&-\bar{n}(\omega_k)[\tilde{\rho}_{\rm S},\tilde{\sigma}_-^{(i)}\tilde{\sigma}_+^{(j)}]\big\},\end{aligned} \tag{A5}$$

where

$$\bar{n}(\omega_k)=\frac{1}{\mathrm{e}^{\beta\omega_k}-1},\ \Gamma_{ij}=2\mathrm{Re}[I_{ij}],\ \Lambda_{ij}=\mathrm{Im}[I_{ij}], \tag{A6}$$

with

$$\begin{aligned}I_{ij}=&\int_0^t\mathrm{d}t'\sum_k g_{i,k}g_{j,k}\mathrm{e}^{\pm\mathrm{i}\Delta\omega_k(t-t')}\\\approx&\sum_k g_{i,k}g_{j,k}\Big[\pi\delta(\Delta\omega_k)\pm\mathrm{i}P\Big(\frac{1}{\Delta\omega_k}\Big)\Big].\end{aligned} \tag{A7}$$

Note that $\Gamma_{ij}\propto\sum_k g_{i,k}g_{j,k}\delta(\omega_k-\omega_0)$ generally depends on the distance between atoms.[32] Considering $\Gamma_{ij}=\Gamma$ and $\Lambda_{ij}=0$ (i.e., the collective spontaneous emissions), we obtain the master equation

$$\begin{aligned}\frac{\mathrm{d}\tilde{\rho}_{\rm S}}{\mathrm{d}t}=&\Gamma\sum_{i,j}\Big[\bar{n}\Big(\tilde{\sigma}_+^{(i)}\tilde{\rho}_{\rm S}\tilde{\sigma}_-^{(j)}-\frac{1}{2}\{\tilde{\rho}_{\rm S},\tilde{\sigma}_-^{(i)}\tilde{\sigma}_+^{(j)}\}\Big)\\&+(\bar{n}+1)\Big(\tilde{\sigma}_-^{(i)}\tilde{\rho}_{\rm S}\tilde{\sigma}_+^{(j)}-\frac{1}{2}\{\tilde{\rho}_{\rm S},\tilde{\sigma}_+^{(i)}\tilde{\sigma}_-^{(j)}\}\Big)\Big],\end{aligned} \tag{A8}$$

where we introduce

$$\bar{n}\equiv\bar{n}(\omega_0)=\frac{1}{\mathrm{e}^{\beta\omega_0}-1}. \tag{A9}$$

Finally, we return to the original rotating frame

$$\begin{aligned}\frac{\mathrm{d}\hat{\rho}}{\mathrm{d}t}=&\frac{\mathrm{d}}{\mathrm{d}t}\big(\mathrm{e}^{-\mathrm{i}\hat{H}_0t}\tilde{\rho}_{\rm S}\,\mathrm{e}^{\mathrm{i}\hat{H}_0t}\big)=-\mathrm{i}[\hat{H}_0,\hat{\rho}]+\mathrm{e}^{-\mathrm{i}\hat{H}_0t}\frac{d\tilde{\rho}_{\rm S}}{dt}\,\mathrm{e}^{\mathrm{i}\hat{H}_0t}\\=&-\mathrm{i}\frac{\lambda}{2}\sum_j[\hat{\sigma}_x^{(j)},\hat{\rho}]\\&+\Gamma\sum_{i,j}\Big[\bar{n}\Big(\hat{\sigma}_+^{(i)}\hat{\rho}\hat{\sigma}_-^{(j)}-\frac{1}{2}\{\hat{\rho},\hat{\sigma}_-^{(i)}\hat{\sigma}_+^{(j)}\}\Big)\\&+(\bar{n}+1)\Big(\hat{\sigma}_-^{(i)}\hat{\rho}\hat{\sigma}_+^{(j)}-\frac{1}{2}\{\hat{\rho},\hat{\sigma}_+^{(i)}\hat{\sigma}_-^{(j)}\}\Big)\Big],\end{aligned} \tag{A10}$$

which can be rewritten as Eq. (11) in the main text. For the case $N=1$, it becomes Eq. (6) in main text.

Appendix B: Analytical results for the single-atom case

For the case $N=1$, we first consider a thermal bath, by taking the density matrix $\hat{\rho}$ as

$$\hat{\rho}=\begin{pmatrix}z+\frac{1}{2} & x+\mathrm{i}y\\ x-\mathrm{i}y & \frac{1}{2}-z\end{pmatrix}, \tag{B1}$$

where we use short-hand notations $x(t)=x$, $y(t)=y$, and $z(t)=z$, with $x,\,y,\,z\in\mathbb{R}$. Considering the initial state $\hat{\rho}_0=\hat{\rho}(0)=\mathrm{e}^{-\beta\hat{H}_{\rm S}}/Z$, we have $x(0)=y(0)=0$, and $z(0)=a_1+b_1$, where

$$\begin{aligned}&a_1=-\frac{\Gamma^2\chi}{2A^2},\ \ b_1=-\frac{\lambda^2}{\chi A^2},\\&A=\sqrt{2\lambda^2+\Gamma^2\chi^2},\ \ \chi=2\bar{n}+1.\end{aligned} \tag{B2}$$

Substituting Eq. (B2) into Eq. (6), we obtain the differential equations

$$\begin{aligned}\dot{x}=&-\frac{\Gamma\chi}{2}x,\\\dot{y}=&-\frac{\Gamma\chi}{2}y+\lambda z,\\\dot{z}=&-\frac{\Gamma}{2}-\Gamma\chi z-\lambda y,\end{aligned} \tag{B3}$$

we obtain

$$\begin{aligned}x=&\,0,\\y=&\,a_2+\mathrm{e}^{-\frac{3}{4}\chi\Gamma t}[b_2\cos(\Omega t)+c_2\sin(\Omega t)],\\z=&\,a_1+\mathrm{e}^{-\frac{3}{4}\chi\Gamma t}[b_1\cos(\Omega t)+c_1\sin(\Omega t)],\end{aligned} \tag{B4}$$

where

$$\begin{aligned}&c_1=-\frac{3\lambda^2\Gamma}{4\Omega A^2},\ c_2=\frac{-4\lambda^3+\lambda\Gamma^2\chi^2}{4\chi\Omega A^2},\\&a_2=-b_2=-\frac{\lambda\Gamma}{A^2},\\&\Omega=\frac{1}{4}\sqrt{16\lambda^2-\chi^2\Gamma^2}.\end{aligned} \tag{B5}$$

Note that

$$\begin{aligned}E(t)=&\,\mathrm{Tr}[\hat{\rho}(t)\hat{H}_{\rm S}]=\omega_0z\\=&\,\omega_0\{a_1+\mathrm{e}^{-\frac{3}{4}\chi\Gamma t}[b_1\cos(\Omega t)+c_1\sin(\Omega t)]\}.\end{aligned} \tag{B6}$$

In the limit $t \to \infty$, the system approaches to a steady state

$$\hat{\rho}(\infty) = \begin{pmatrix} a_1 + \frac{1}{2} & \mathrm{i}a_2 \\ -\mathrm{i}a_2 & \frac{1}{2} - a_1 \end{pmatrix}. \tag{B7}$$

We diagonalize $\hat{\rho}(\infty)$ and obtain the passive state

$$\begin{aligned} \hat{\sigma}_{\mathrm{p}} &= \frac{1}{2}\hat{I} - \sqrt{a_1^2 + a_2^2}\hat{\sigma}_z \\ &= \frac{1}{2}\hat{I} - \frac{\Gamma\sqrt{4\lambda^2 + \chi^2\Gamma^2}}{4A^2}\hat{\sigma}_z, \end{aligned} \tag{B8}$$

where $\hat{I}$ is the identity matrix and $\hat{\sigma}_z$ is the Pauli-z matrix. Hence, we obtain the ergotropy W, as Eq. (8) in the main text.

Acknowledgments

Project supported by the National Natural Science Foundation of China (Grant Nos. 12075209, 11905185, and 11935012) and partially supported by the Science Foundation of Zhejiang Sci-Tech University (Grant No. 18062145-Y).

References

[1] Bhattacharjee S and Dutta A 2021 *J. Phys. A: Math. Theor.* **94** 239
[2] Binder F, Correa L A, Gogolin C, Anders J and Adesso G E 2018 *Thermodynamics in the Quantum Regime (Fundamental Aspects and New Directions)* (Berlin: Springer) p. 207
[3] Kamin F H, Tabesh F T, Salimi S and Santos A C 2020 *Phys. Rev. E* **102** 052109
[4] Rossini D, Andolina G M, Rosa D, Carrega M and Polini M 2020 *Phys. Rev. Lett.* **125** 236402
[5] Gyhm J Y, Šafránek D and Rosa D 2022 *Phys. Rev. Lett.* **128** 140501
[6] Alicki R and Fannes M 2013 *Phys. Rev. E* **87** 042123
[7] Hovhannisyan K V, Perarnau-Llobet M, Huber M and Acín A 2013 *Phys. Rev. Lett.* **111** 240401
[8] Andolina G M, Keck M, Mari A, Giovannetti V and Polini M 2019 *Phys. Rev. B* **99** 205437
[9] Peng L, He W B, Chesi S, Lin H Q and Guan X W 2021 *Phys. Rev. A* **103** 052220
[10] Le T P, Levinsen J, Modi K, Parish M M and Pollock F A 2018 *Phys. Rev. A* **97** 022106
[11] Julià-Farré S, Salamon T, Riera A, Bera M N and Lewenstein M 2020 *Phys. Rev. Res.* **2** 023113
[12] Seah S, Perarnau-Llobet M, Haack G, Brunner N and Nimmrichter S 2021 *Phys. Rev. Lett.* **127** 100601
[13] Chen P, Yin T S, Jiang Z Q and Jin G R 2022 *Phys. Rev. E* **106** 054119
[14] Shaghaghi V, Singh V, Benenti G and Rosa D 2022 *Quantum Sci. Technol.* **7** 04LT01
[15] Salvia R, Perarnau-Llobet M, Haack G, Brunner N and Nimmrichter S 2023 *Phys. Rev. Res.* **5** 013155
[16] Levy A, Diosi L and Kosloff R 2016 *Phys. Rev. A* **93** 052119
[17] Seah S, Nimmrichter S and Scarani V 2018 *New J. Phys.* **20** 043045
[18] Ferraro D, Campisi M, Andolina G M, Pellegrini V and Polini M 2018 *Phys. Rev. Lett.* **120** 117702
[19] Andolina G M, Farina D, Mari A, Pellegrini V, Giovannetti V and Polini M 2018 *Phys. Rev. B* **98** 205423
[20] Andolina G M, Keck M, Mari A, Campisi M, Giovannetti V and Polini M 2019 *Phys. Rev. Lett.* **122** 047702
[21] Monsel J, Fellous-Asiani M, Huard B and Auffèves A 2020 *Phys. Rev. Lett.* **124** 130601
[22] Crescente A, Carrega M, Sassetti M and Ferraro D 2020 *Phy. Rev. B* **102** 245407
[23] Quach J Q, McGhee K E, Ganzer L, Rouse D M, Lovett B W, Gauger E M, Keeling J, Cerullo G, Lidzey D G and Virgili T 2022 *Sci. Adv.* **8** eabk3160
[24] Binder F C, Vinjanampathy S, Modi K and Goold J 2015 *New J. Phys.* **17** 075015
[25] Campaioli F, Pollock F A, Binder F C, Céleri L, Goold J, Vinjanampathy S and Modi K 2017 *Phys. Rev. Lett.* **118** 150601
[26] Fusco L, Paternostro M and De Chiara G 2016 *Phys. Rev. E* **94** 052122
[27] Farina D, Andolina G M, Mari A, Polini M and Giovannetti V 2019 *Phys. Rev. B* **99** 035421
[28] Zhang Y Y, Yang T R, Fu L and Wang X G 2019 *Phys. Rev. E* **99** 052106
[29] Chang W, Yang T R, Dong H, Fu L, Wang X G and Zhang Y Y 2021 *New J. Phys.* **23** 103026
[30] Allahverdyan A E, Balian R and Nieuwenhuizen Th M 2004 *Europhys. Lett.* **67** 565
[31] Johansson J R, Nation P D and Nori F 2012 *Comput. Phys. Commun.* **183** 1760
[32] Ficek Z and Swain S 2005 *Quantum Interference and Coherence* (New York: Springer) p. 62